Langmuir

ARTICLE

pubs.acs.org/Langmuir

Effect of Salt on the Equilibrium and Nonequilibrium Features of Polyelectrolyte/Surfactant Association

Katalin Pojják, Edit Bertalanits, and Róbert Mészáros*

Laboratory of Interfaces and Nanosized Systems, Institute of Chemistry, Eötvös Loránd University, 1117 Budapest, Pázmány Péter Sétány 1/A, Hungary

Supporting Information

ABSTRACT: The impact of an electrolyte on aqueous mixtures of oppositely charged macromolecules and surfactants is usually explained by assuming an equilibrium association between the components. In this work, it is shown that the nonequilibrium character of polyelectrolyte/surfactant systems plays a crucial role in the interpretation of the effect of salt. Experimental investigations of mixtures of sodium poly(styrenesulfonate) (PSS) and hexadecyltrimethylammonium bromide (CTAB) reveal two distinct effects of added sodium chloride (NaCl). At small and moderate NaCl concentrations, the major impact of the electrolyte is manifested in the reduction of the kinetically stable composition range in which the PSS/CTAB mixtures are trapped in the nonequilibrium colloidal dispersion state. The application of high salt concentrations, however, primarily affects the equilibrium phase properties through considerably decreasing the amount of surfactant bound to the polyelectrolyte.

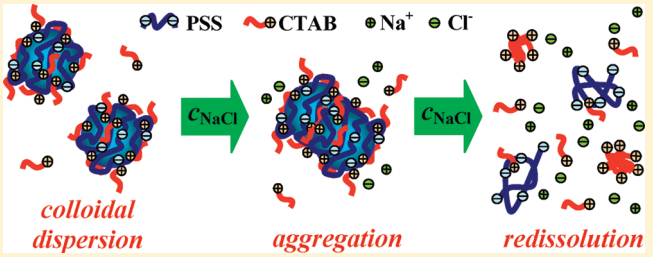

INTRODUCTION

During the use of various applications based on oppositely charged macromolecules and amphiphiles,[1−3] the ionic strength may vary significantly. Therefore, many studies were carried out to understand the impact of supporting electrolytes on the polyelectrolyte/surfactant association.[4−16] One of the most important effects of salt is its influence on the phase behavior of polyelectrolyte/surfactant mixtures. In the absence of electrolyte, associative phase separation occurs at intermediate surfactant-to-polyelectrolyte ratios.[17,18] The associative term means that one of the two phases is enriched in both the polyelectrolyte and the surfactant components. At higher and lower surfactant-to-polyelectrolyte ratios, the formation of transparent systems is reported in the salt-free systems.[19,20] Another type of precipitation can be observed in a certain composition range in the presence of suitably high salt concentrations.[6−8,17] In this case, a so-called segregative phase separation into one polyelectrolyte-rich and one surfactant-rich phase takes place.[17]

However, the impact of electrolyte on the bulk behavior is rather complex at relatively low and intermediate salt concentrations (which are more relevant with respect to the practical applications). The studies discussing this salt concentration range can be divided into three main groups. Thalberg and co-workers found that above a critical electrolyte concentration (cec) the addition of salt completely suppresses the two-phase concentration region for mixtures of sodium polyacrylate and sodium hyaluronate with different alkyltrimethylammonium bromides.[4−6] In contrast, the broadening of the precipitation concentration range with increasing salt concentration was observed for mixtures of sodium dodecyl sulfate (SDS) with various cationic polyelectrolytes including poly(ethyleneimine) (PEI),[7] poly(vinylamine),[8] and poly(diallyldimethylammonium chloride).[8] Another group of studies revealed two opposite effects of added salt on the phase properties. Voisin and Vincent reported the enhancement of the two-phase composition range with increasing sodium chloride (NaCl) concentration for the mixtures of sodium lauryl ether sulfate and cationic polyelectrolyte "Jaguar".[9] However, at significantly higher NaCl concentrations, the authors observed the complete suppression of the precipitation concentration region.[9] Similar observations were made for mixtures of different cationic surfactants with sodium carboxymethylcellulose as well as with a neutral anionic block copolymer.[10,12,13]

The above-mentioned examples illustrate that the dependence of the polyelectrolyte/surfactant association on the salt concentration is far from being understood. In this work, we aim to rationalize the impact of electrolyte on the bulk behavior of polyelectrolyte/surfactant systems. In our experiments, aqueous mixtures of hexadecyltrimethylammonium bromide (CTAB) with two sodium poly(styrenesulfonate) (PSS) samples of different molecular masses are investigated in the absence and presence of NaCl. The apparent mean size and the charged nature of the PSS/CTAB complexes are characterized by means of dynamic light scattering and electrophoretic mobility measurements. The aggregation of the complexes is monitored by coagulation kinetics experiments. The results are also compared with observations on the poly(ethyleneimine)/sodium dodecyl sulfate system in the presence of salt.

Received: March 5, 2011
Published: June 24, 2011

EXPERIMENTAL SECTION

Materials. High- and low-molecular-mass sodium poly(styrenesulfonate) (PSS, Sigma-Aldrich, $M_{w,PSS} = 10^6$ and 7×10^4 Da) was purchased in powder form. The stock solution of the high-molecular mass PSS sample was purified by dialysis. Hexadecytrimethylammonium bromide (CTAB, Sigma-Aldrich) was recrystallized from a 1:1 benzene−acetone mixture, and its cmc was found to be 0.92 mM (without added salt) at 25.0 ± 0.1 °C on the basis of conductivity measurements. The applied supporting electrolyte was sodium chloride (NaCl, Sigma-Aldrich). For the sake of comparison, a few experiments were also performed on mixtures of poly(ethyleneimine) (PEI, Sigma-Aldrich, $M_{w,PEI} = 7.5 \times 10^5$ Da, in 50 wt % solution) and sodium dodecyl sulfate (SDS, Sigma-Aldrich). The PEI stock solution was purified by mixed bed cation/anion exchange and dialysis. ACS reagent-grade HCl and NaOH (Sigma-Aldrich) were used to adjust the initial pH of the PEI solutions (which is denoted as pH^{in} throughout the article). The SDS sample was recrystallized twice from a 1:1 benzene−ethanol mixture, and its cmc was 8.1 mM (in the absence of salt) at 25.0 ± 0.1 °C as determined from conductivity measurements. During the experiments, ultraclean Milli-Q water (Milli-Q Integral 3 system) was used for solution preparation.

Preparation of the Polyelectrolyte/Surfactant Systems. The PSS/CTAB mixtures without added salt were prepared by making use of one of the two following mixing protocols.

Stop-Flow Mixing. Equal volumes of surfactant and polyelectrolyte solutions were mixed by means of an Applied Photophysics (model RX 1000) stop-flow apparatus. This mixing method is very efficient because the two solutions are mixed within 10 ms.[21,22]

Slow Mixing. In the slow-mixing protocol, equal volumes of polyelectrolyte and surfactant solutions were mixed, but the surfactant solution was added very slowly, drop by drop, to the polyelectrolyte solution under continuous stirring with a magnetic stirrer. A similar mixing method was applied in ref 23.

In the case of added salt, the preparation of the PSS/CTAB mixtures was carried out in three different ways.

Stop-Flow Mixing in Salt. Equal volumes of surfactant and polyelectrolyte solutions (both of which contained the same amount of NaCl) were mixed by the stop-flow-mixing protocol described above. A majority of the polyelectrolyte/surfactant mixtures was prepared by this mixing method in the presence of salt.

Two-Step Mixing in Salt I. The final composition of the system was attained in two steps. First, equal volumes of surfactant and polyelectrolyte solutions were mixed by the slow-mixing protocol described above where none of the solutions contained added NaCl. These mixtures were left to stand for a day at room temperature. Next, to attain the final composition, the systems were mixed with concentrated NaCl solution in equal volumes and stirred with a magnetic stirrer for a day.

Two-Step Mixing in Salt II. Similar to the previous mixing method, the final composition of the systems was attained in two steps. First, equal volumes of surfactant and polyelectrolyte solutions were mixed by the slow-mixing protocol, where none of the solutions contained added NaCl. These mixtures were left to stand for a day at room temperature. Next, solid NaCl crystals were added to the mixtures, and the systems were stirred by a magnetic stirrer for a day. In this case, the dissolution of NaCl results in an approximately 3% reduction in the concentrations of PSS and CTAB (whose concentration change was neglected).

The preparation of the PSS/CTAB mixtures via the mentioned different mixing methods in the presence of salt is illustrated in Scheme 1 of the Supporting Information.

METHODS

Electrophoretic Mobility Measurements. The mean electrophoretic mobility (u_ζ) of the samples was determined at 25.0 ± 0.1 °C, 24 h after solution preparation using a Malvern Zetasizer Nano Z instrument. The apparatus uses the M3-PALS technique, which is a combination of laser Doppler velocimetry and phase analysis light scattering methods. The relative standard error of the mean electrophoretic mobility was around 5−10%.

Dynamic Light Scattering Measurements. The light scattering measurements were performed by means of Brookhaven equipment consisting of a BI-200SM goniometer system and a BI-9000AT digital correlator. The measurements were carried out at a $\theta = 90°$ scattering angle and at 25.0 ± 0.1 °C, 24 h after solution preparation. The light source was an argon ion laser (Omnichrome, model 543AP) operating at a 488 nm wavelength and emitting vertically polarized light. The intensity−intensity time-correlation functions were measured (homodyne method) and then converted by means of the Siegert relation to the normalized electric field autocorrelation functions. The autocorrelation functions were analyzed by the second-order cumulant expansion and the CONTIN methods. The investigated PSS and PEI samples were found to be polydisperse with wide unimodal distributions. As indicated by the CONTIN analysis, the addition of surfactant does not change the character of the size distribution of the polyelectrolyte molecules significantly. The apparent diffusion coefficient (D_{app}) of the polyelectrolyte/surfactant complexes in the presence and absence of NaCl was derived from the mean relaxation rate ($\Gamma(q)$, first cumulant)

$$D_{app}(q) = \frac{\Gamma(q)}{q^2} \tag{1}$$

where q is the scattering vector ($q = (4\pi n/\lambda_o)\sin(\theta/2)$, n is the refractive index of the solution, and λ_o is the wavelength of the incident light). The apparent mean hydrodynamic diameter (d_H) of the complexes was calculated from D_{app} according to the Einstein−Stokes relation

$$D_{app} = \frac{k_B T}{3\pi\eta d_H} \tag{2}$$

where k_B is the Boltzmann constant, T is the absolute temperature, and η is the viscosity of the medium. Prior to the measurements, the solutions were filtered through 0.8 μm pore-size membrane filters.

Coagulation Kinetics Measurements. The initial rate of coagulation of the PSS/CTAB and PEI/SDS nanoparticles formed in the presence of excess surfactant was determined at 25.0 ± 0.1 °C using a Perkin-Elmer (Lambda 2) spectrophotometer coupled with a stop-flow-mixing unit (model RX 1000, Applied Photophysics Ltd.). First, the polyelectrolyte/surfactant mixtures were prepared via the stop-flow-mixing protocol and left to stand for 24 h. Next, these systems were mixed with NaCl solutions in equal volumes using the stop-flow equipment, and the absorbance (Ab) versus time (t) curves were monitored at 480 nm.

In the case of monodisperse colloidal particles, the initial rate of coagulation can be approximated by second-order kinetics

$$-\frac{dN}{dt} = kN^2 \tag{3}$$

where k is the absolute coagulation rate constant and N is the number of particles per unit volume.

The experimental coagulation rate constant (k^x) can be determined according to the Oster equation from the initial slope of the absorbance versus time curves provided that the size of the particles is small compared to the wavelength of the light beam[9,24]

$$\left[\frac{dAb}{dt}\right]_{t \to 0} = k^x = 2lA'N_0^2V_0^2k \tag{4}$$

where l is the optical path length and N_0 and V_0 denote the concentration and volume of the primary particles, respectively, at the beginning of the coagulation process. A' is a constant that depends on the wavelength of the incident beam and the refractive indices of the particles and the medium. Typical examples of the variation of absorbance with time for

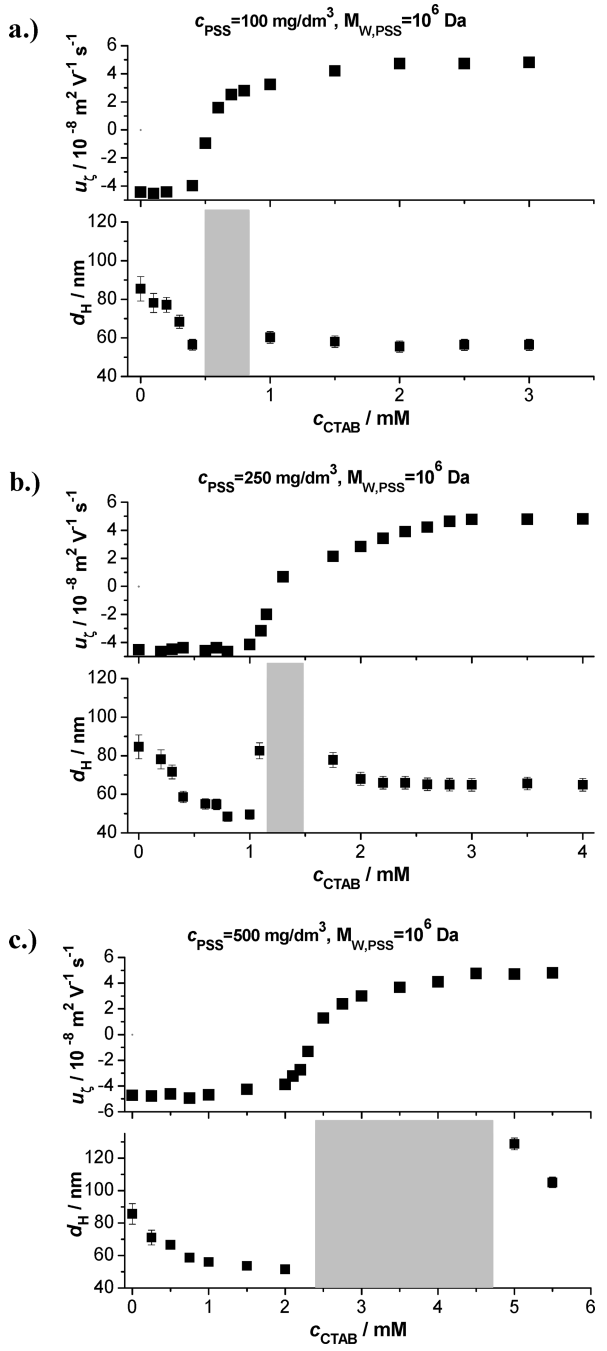

Figure 1. Mean electrophoretic mobility (u_ζ) and apparent mean hydrodynamic diameter (d_H) of the PSS/CTAB complexes against the analytical CTAB concentration. $M_{W,PSS}$ = 10^6 Da: (a) c_{PSS} = 100 mg/dm^3, (b) c_{PSS} = 250 mg/dm^3, and (c) c_{PSS} = 500 mg/dm^3. The mixtures were prepared via the stop-flow-mixing protocol. The gray area indicates the composition range of precipitated and/or very turbid systems. The standard error of the mobility values is commensurate with the size of the symbols.

PSS/CTAB systems in the presence of salt are shown in Figure S1 in the Supporting Information.

RESULTS AND DISCUSSION

Association between PSS and CTAB without Added Salt. We begin our examination with the characterization of the complexation between PSS and CTAB in the absence of added NaCl. In Figure 1a−c, the mean electrophoretic mobility (u_ζ) and the apparent mean hydrodynamic diameter (d_H) of the PSS/CTAB complexes are plotted against the analytical CTAB concentration at different fixed concentrations of the high-molecular-mass PSS sample ($M_{w,PSS}$ = 10^6, c_{PSS} = 100, 250, and 500 mg/dm^3). These mixtures were prepared via the stop-flow-mixing protocol, which ensures a very rapid homogenization of the system.

As shown in the figures, the mobility of the complexes varies in a similar fashion with the surfactant concentration at each investigated PSS concentration. Because of the binding of the cationic surfactant, the initial negative charge density of the PSS molecules decreases with increasing CTAB concentration. The charge neutralization of the complexes occurs at approximately the stoichiometric mixing ratios of the polyelectrolyte charges and the cationic surfactant molecules. (The complete dissociation of the sodium styrene sulfonate monomers would result in approximately 4.8 mmol of charged segments/g of PSS, which amounts to 0.48, 1.2, and 2.4 mM CTAB upon stoichiometric mixing at c_{PSS} = 100, 250, and 500 mg/dm^3, respectively, in accordance with our measurements.) In the vicinity of these composition regions, precipitation occurs.

A further increase in the surfactant concentration leads to the charge reversal of the PSS/CTAB complexes. In the presence of excess surfactant, the mobility and therefore the positive charge density of the complexes increase with increasing CTAB concentration and the formation of transparent systems can be observed again. Because of the appearance of free micelles, u_ζ levels off at $u_\zeta^{cmc} \approx 4.8 \pm 0.2$ (10^{-8} m^2 V^{-1} s^{-1}) for each PSS concentration. Similar mobility versus surfactant concentration curves to those in Figure 1a−c were observed for the previously investigated polycation/SDS systems at constant polyelectrolyte concentrations.[7,8,21−23,25]

According to Figure 1a−c, the variation of the apparent mean hydrodynamic diameter of the PSS/CTAB complexes with the total surfactant concentration as well as the width of the precipitation concentration range reveals a marked dependence on the polyelectrolyte concentration. In the transparent preprecipitation concentration range (excess polyelectrolyte), the apparent mean size of the complexes decreases with increasing CTAB concentration at each PSS concentration because of the decreasing charge density of the PSS/CTAB complexes. However, the intermediate surfactant concentration range, where precipitation and/or the formation of very turbid systems are observed, is much larger at c_{PSS} = 500 mg/dm^3 than at the two lower PSS concentrations. Furthermore, at 100 and 250 mg/dm^3 PSS concentrations, transparent mixtures with low but visually observable turbidity are formed in the presence of excess surfactant. These mixtures contain positively charged polyelectrolyte/surfactant complexes of roughly the same size (d_H = 56 ± 3 nm and 65 ± 3 nm at c_{PSS}= 100 and 250 mg/dm^3, respectively) over a wide composition range. In contrast, at 500 mg/dm^3 PSS concentration transparent systems can be observed in a considerably narrower concentration range in the presence of excess surfactant. Moreover, in these latter mixtures the apparent mean size of the complexes is larger (d_H > 100 nm) than that of the surfactant-free polyelectrolyte molecules (85 ± 6 nm).

In Figure 2, the mean electrophoretic mobility and apparent mean hydrodynamic diameter of the complexes are shown as a function of the analytical surfactant concentration for the low-molecular-mass PSS sample ($M_{w,PSS}$ = 7 × 10^4 Da, c_{PSS} = 250 mg/dm^3,

dx.doi.org/10.1021/la2021353 |Langmuir 2011, 27, 9139–9147

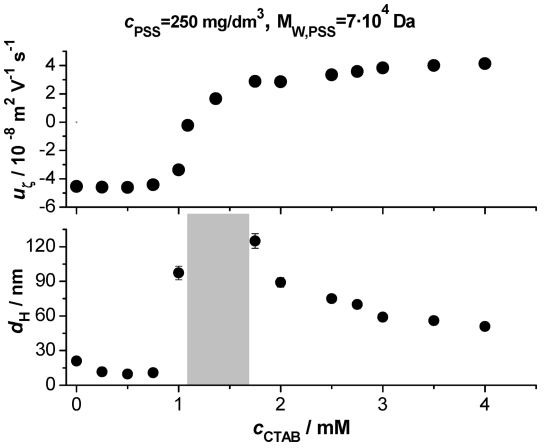

Figure 2. Mean electrophoretic mobility (u_ζ) and apparent mean hydrodynamic diameter (d_H) of the PSS/CTAB complexes against the analytical CTAB concentration. $M_{w,PSS}$ = 7 × 10^4 Da and c_{PSS}= 250 mg/dm^3. The mixtures were prepared via the stop-flow-mixing protocol. The gray area indicates the composition range of precipitated and/or very turbid systems. The standard error of the mobility values is commensurate with the size of the symbols.

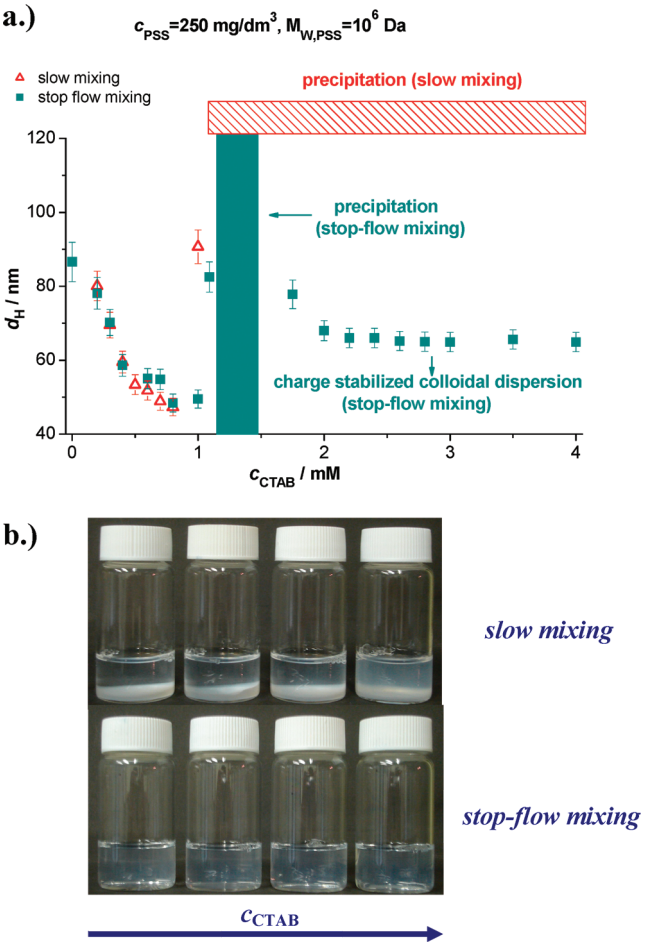

Figure 3. (a) Effect of the applied mixing protocol on the apparent mean hydrodynamic diameter versus surfactant concentration curves. Key: stop-flow-mixing (green ■); slow-mixing (red △). $M_{w,PSS}$ = 10^6 Da and c_{PSS}= 250 mg/dm^3. The green filled and the red sparse areas indicate the composition range of precipitated systems belonging to the mixtures made by stop-flow-mixing and slow-mixing, respectively. (b) Photograph of the PSS/CTAB systems prepared by the two mixing methods in excess CTAB. (Top row) Slow-mixing procedure. (Bottom row) Stop-flow-mixing procedure. The concentration of CTAB increases from left to right as follows: 2.5, 3.0, 3.5, and 4.0 mM CTAB. $M_{w,PSS}$ = 10^6 Da and c_{PSS}= 250 mg/dm^3.

the mixtures were prepared by the stop-flow-mixing protocol). The u_ζ versus c_{CTAB} curve is very similar to the one measured for the high-molecular-mass PSS sample at the same polyelectrolyte concentration (Figure 1b). The only difference is that the maximum value of the electrophoretic mobility measured at a large excess of surfactant is lower for the smaller-chain-length PSS sample ($u_\zeta^{cmc} \approx 4.0 \pm 0.2$ and 4.8 ± 0.2 (10^{-8} m^2 V^{-1} s^{-1}) for $M_{w,PSS}$ = 7 × 10^4 and $M_{w,PSS}$ = 10^6 Da, respectively).

Similar to the high-molecular-mass PSS sample at c_{PSS} = 250 mg/dm^3, the apparent mean size of the PSS/CTAB complexes decreases with increasing CTAB concentration in the presence of excess polyelectrolyte, and transparent systems are formed over a wide composition range of excess surfactant. However, a significant deviation compared to the results in Figure 1b is that in Figure 2 the observed d_H values of the complexes formed in the presence of excess surfactant are much larger (d_H > 50 nm) than the apparent mean size of the pure polyelectrolyte molecules (21 ± 3 nm). Furthermore, the width of the precipitation concentration range is larger for the low-molecular-mass PSS sample than for the high-molecular-mass PSS sample at c_{PSS} = 250 mg/dm^3.

Nonequilibrium Features of PSS/CTAB Association. Within the classical framework of equilibrium polyelectrolyte/surfactant association, the transparent systems in Figures 1a−c and 2 (at low and high CTAB concentrations) would be considered to be thermodynamically stable one-phase systems. However, the oppositely charged macromolecule/surfactant mixtures are frequently reported to be trapped in nonequilibrium states.[21−23,26−31] To test the thermodynamic stability of the PSS/CTAB mixtures, the systems at the investigated compositions in Figures 1a−c and 2 were also prepared by the slow-mixing protocol in which the CTAB solution is added slowly, in a dropwise manner, to an equal volume of PSS solution.

In Figure 3, the effect of the two kinds of solution preparation methods on the apparent mean size of the PSS/CTAB complexes is shown for the high-molecular-mass PSS sample at 250 mg/dm^3 polyelectrolyte concentration. At low surfactant-to-polyelectrolyte ratios, the applied mixing protocols give roughly the same mean diameter of the complexes except in a narrow CTAB concentration range close to the charge neutralization. In this latter composition range, the apparent mean size of the complexes is larger and precipitation can be observed at a slightly lower surfactant concentration for the slow-mixing than for the stop-flow-mixing protocol. At high surfactant-to-polyelectrolyte ratios, however, a dramatic effect of the mixing method is observable. Contrary to the transparent systems of positively charged complexes formed by the application of the stop-flow-mixing protocol (bottom row in the photograph in Figure 3b), precipitation occurs for the PSS/CTAB mixtures prepared via the slow-mixing procedure (top row in the photograph in Figure 3b). These precipitates cannot be dissolved even by continuous stirring with a magnetic stirrer for a long time (weeks). The same results were observed at the two other concentrations of the high-molecular-mass PSS sample as well as at the same monomer concentration of the low-molecular-mass PSS sample (Figure S2 ($M_{w,PSS}$ = 10^6 Da, c_{PSS} = 100 mg/dm^3), S3 ($M_{w,PSS}$ = 10^6 Da,

dx.doi.org/10.1021/la2021353 |*Langmuir* 2011, 27, 9139–9147

c_{PSS} = 500 mg/dm^3), and S4 ($M_{w,PSS}$ =7 × 10^4 Da, c_{PSS} = 250 mg/dm^3) in the Supporting Information).

The different states of the PSS/CTAB mixtures at a given composition (precipitated for slow-mixing and transparent for stop-flow-mixing) still persist. These findings clearly demonstrate that the PSS/CTAB systems may not be in thermodynamic equilibrium in the given concentration range of excess surfactant.

In recent work, it was shown that the nonequilibrium complexation between SDS and various cationic polyelectrolytes is attributable to the formation of electrostatically stabilized colloidal dispersions of polyelectrolyte/surfactant nanoparticles in the presence of excess surfactant.[7,8,21−23,30,31] The kinetic stability of these dispersions is ensured by the adsorption of surfactant ions on the surface of the polyelectrolyte/surfactant nanoparticles.[7,8,21−23,30−32]

In light of this reasoning, a possible explanation for the results in Figure 3 and Figures S2−S4 is that in the investigated composition range of excess surfactant the PSS/CTAB mixtures would form two-phase systems in equilibrium. However, through the application of the very rapid mixing of the components, the aggregation of the formed nanophases of the insoluble polyelectrolyte/surfactant salt (to which we also refer to as PSS/CTAB nanoparticles in the following text) is considerably hindered if the adsorption of the cationic surfactant considerably charges the surface of these nanoparticles. Therefore, macroscopic (associative) phase separation cannot be observed because at sufficiently large surfactant-to-polyelectrolyte ratios the PSS/CTAB mixtures are trapped in the charge-stabilized, nonequilibrium colloidal dispersion state.

In contrast, when the surfactant solution is added gradually to the polyelectrolyte solution, the slightly charged primary PSS/CTAB nanoparticles, formed in the intermediate stage of the slow-mixing procedure, coagulate. This aggregation process and the subsequent sedimentation of the large aggregates result in phase separation. The precipitate cannot be redispersed upon further addition of the CTAB solution because the adsorption of the surfactant ions cannot disaggregate the irreversibly coagulated PSS/CTAB nanoparticles. Eventually, an equilibrium macroscopic two-phase system is formed in the investigated composition range of excess surfactant. In the presence of excess polyelectrolyte, the effect of mixing is less pronounced because the system does not go through the unstable states of electroneutral polyelectrolyte/surfactant complexes.

Impact of the Concentration and Molecular Mass of the Polyelectrolyte. The formation of charge-stabilized colloidal dispersions in the presence of excess surfactant in the case of the stop-flow-mixing protocol is also reflected by the earlier shown dependence of the apparent mean size of the PSS/CTAB complexes on the concentration and molecular mass of the PSS samples in Figures 1a−c and 2. Recently, it was shown that the apparent mean diameter of polycation/SDS complexes, formed in the electrostatically stabilized colloidal dispersion composition range, is strongly affected by the polyelectrolyte concentration.[21,22]

The apparent mean size of the polyelectrolyte/surfactant nanoparticles and the width of the kinetically stable composition range of their colloidal dispersion are determined by the extent of local coagulation of the primary polyelectrolyte/surfactant complexes, which is induced by the local inhomogeneities developed in the initial stage of the mixing process.[21,22] The initial rate of this local aggregation process is roughly proportional to the square of the molar concentration of the individual polyelectrolyte chains. This explains the largely increased precipitation concentration

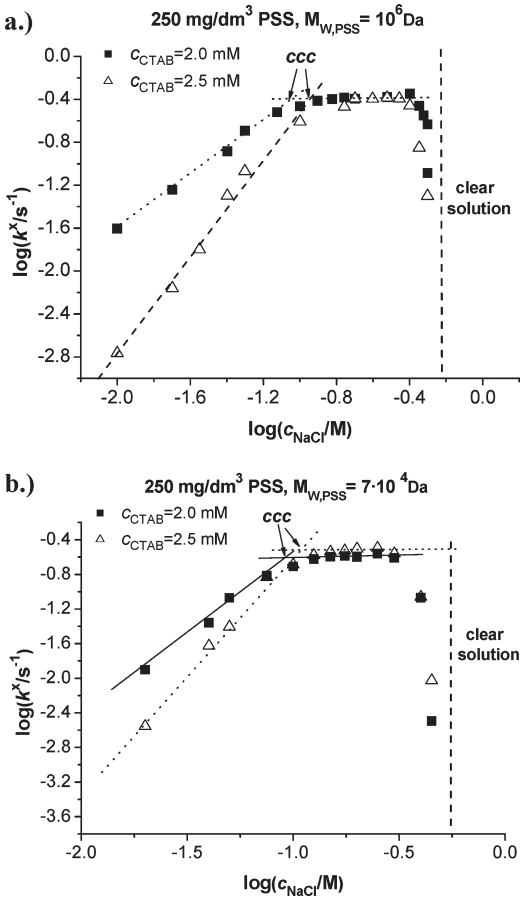

Figure 4. Logarithm of the experimental coagulation rate constant of the positively charged PSS/CTAB nanoparticles as a function of the logarithm of the electrolyte concentration at fixed polyelectrolyte-to-surfactant ratios. First, the PSS/CTAB mixtures were prepared via the application of the stop-flow-mixing protocol and left to stand for 24 h. Next, these systems were mixed with NaCl solutions by stop-flow mixing. (a) $M_{w,PSS}$ = 10^6 Da, c_{PSS}= 250 mg/dm^3, c_{CTAB} = 2.0 mM (■), and 2.5 mM (△). (b) $M_{w,PSS}$ = 7 × 10^4 Da, c_{PSS}= 250 mg/dm^3, c_{CTAB} = 2.0 mM (■), and 2.5 mM (△). The standard error of log(k^x) is commensurate with the size of the symbols.

range and the elevated apparent mean size of the positively charged PSS/CTAB nanoparticles at 500 mg/dm^3 polyelectrolyte concentration compared to the smaller concentrations of the high-molecular-mass PSS sample as shown in Figure 1a−c. Similar effects of the polyelectrolyte concentration were reported for various polycation/SDS systems.[21,22]

However, at a fixed monomer concentration of PSS, another way to increase the molar concentration of the individual polyelectrolyte molecules is to apply macromolecules with smaller chain lengths. Therefore, at c_{PSS} = 250 mg/dm^3 the effect of local inhomogeneities upon mixing is much more pronounced for the low-molecular-mass than for the high-molecular-mass PSS sample. Consequently, as clearly indicated by the comparison of the results in Figures 1b and 2, the PSS/CTAB nanoparticles formed in the presence of excess surfactant contain a considerably larger number of individual polyelectrolyte chains in the case of $M_{w,PSS}$ = 7 × 10^4 Da than for the $M_{w,PSS}$ = 10^6 Da PSS sample. It should be emphasized, however, that the size distribution of the polyelectrolyte/surfactant aggregates cannot be determined because of the polydispersity of the PSS samples.

dx.doi.org/10.1021/la2021353 |Langmuir 2011, 27, 9139–9147

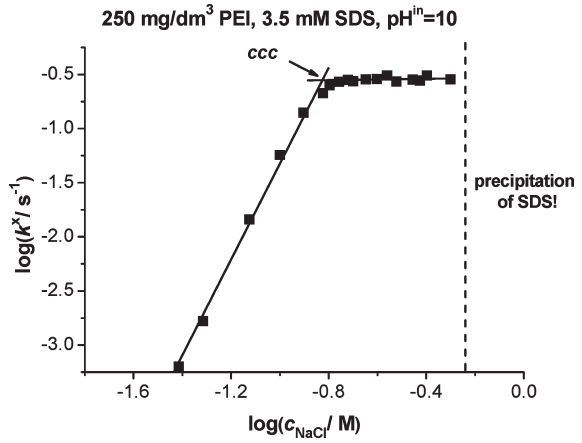

Figure 5. Logarithm of the experimental coagulation rate constant of negatively charged PEI/SDS nanoparticles formed in the presence of excess surfactant against the logarithm of the electrolyte concentration at a given polyelectrolyte-to-surfactant ratio. c_{PEI} = 250 mg/dm^3, c_{SDS} = 3.5 mM, and pH^{in} 10. At $c_{NaCl} \geq 0.6$ M, the precipitation of SDS can be observed in the polyelectrolyte-free solutions. The standard error in $\log(k^x)$ is commensurate with the size of the symbols. The preparation of the polyelectrolyte/surfactant mixtures as well as the addition of salt was carried out in the same way as in the case of Figure 4.

Effect of Salt on the Aggregation of Polyelectrolyte/Surfactant Nanoparticles. If the PSS/CTAB mixtures prepared by the stop-flow-mixing method are electrostatically stabilized colloidal dispersions at high surfactant-to-polyelectrolyte ratios, then their kinetic stability is expected to decrease with increasing ionic strength because of the accelerated aggregation of the polyelectrolyte/surfactant nanoparticles. Figure 4a,b shows the logarithm of the experimental coagulation rate constant of positively charged PSS/CTAB nanoparticles as a function of the logarithm of the NaCl concentration at two surfactant-to-polyelectrolyte ratios for both PSS samples at c_{PSS} = 250 mg/dm^3. With increasing NaCl concentration, the rate of coagulation increases up to the critical coagulation electrolyte concentration (ccc $\approx$ 0.1 M NaCl) and then becomes constant at intermediate salt concentrations. This type of behavior was observed for a variety of polycation/SDS systems[7,8] in the charge-stabilized colloidal dispersion concentration range. In Figure 5, a typical example of the $\log(k^x)$ versus $\log(c_{NaCl})$ curves of PEI/SDS systems in the presence of excess surfactant is shown. (The mixtures were also prepared by stop-flow-mixing.)

The observed impact of added salt on the aggregation rate of PSS/CTAB nanoparticles is qualitatively consistent with the predictions of the DLVO theory for electrostatically stabilized colloidal dispersions. This finding, therefore, clearly reveals that the addition of salt in moderate concentrations primarily affects the nonequilibrium character of polyelectrolyte/surfactant association.

According to Figure 4a,b, with further increases in the NaCl concentration another effect of the added electrolyte on the aggregation rate of PSS/CTAB nanoparticles can be observed, which remarkably deviates from the one described above. Namely, at a given NaCl concentration ($\sim$0.35 M) the initial coagulation rate starts to decrease with increasing salt concentration. At even higher salt concentrations (c_{NaCl} > 0.6 M), coagulation cannot be detected at all because clear solutions with no visible turbidity are formed in the spectrophotometer cuvette. The decreasing coagulation rate of the polyelectrolyte/surfactant nanoparticles as a function of the electrolyte concentration was not detected for the colloidal dispersions of polycation/SDS nanoparticles[7,8] (Figure 5).

The effect of added NaCl on the aggregation rate of PSS/CTAB nanoparticles at high ionic strengths can be rationalized in two different ways. On one hand, because the surface layer of the charged polyelectrolyte/surfactant nanoparticles is hydrophilic as a result of the adsorbed surfactant ions, the diminishing coagulation rate of PSS/CTAB nanoparticles at large salt concentrations may be attributable to the repulsive hydration forces developed between the particles at high ionic strengths. The hydration interactions are closely related to the restructuring of water molecules around the charged colloidal particles induced by the presence of specific ions in the interfacial layer of the particles.[33] These kinds of repulsive interactions are behind the restabilization of the colloidal dispersions of protein-coated polystyrene latex particles in the presence of large electrolyte concentrations.[34] One might argue, therefore, that the PSS/CTAB nanoparticles formed in the presence of excess surfactant without added salt restabilize at high NaCl concentrations. It should be emphasized that this kind of salt effect is strictly related to the kinetic stability of the colloidal dispersions of polyelectrolyte/surfactant nanoparticles by indirectly assuming that the size and internal core of these particles are not dependent on the salt concentration.

On the other hand, the observed impact of electrolyte at high ionic strengths may also be rationalized through its effect on the amount of surfactant bound to the PSS molecules.[35] In the following sections, we will show that this latter type of salt effect is the one that actually accounts for the largely reduced coagulation rate of PSS/CTAB nanoparticles at high NaCl concentrations.

Impact of Electrolyte on the Bound Amount of Surfactant. Theoretical and experimental surfactant binding studies reveal that the onset of surfactant binding shifts to higher equilibrium surfactant concentration and that the driving force of surfactant binding decreases with increasing electrolyte concentration.[35−37] This latter observation is attributed to the decreasing extent of counterion release of the polyelectrolyte molecules with increasing salt concentration, similar to the oppositely charged polyanion/polycation association.[38] Another important effect of the added salt is that it reduces the cmc of the ionic surfactants and therefore the maximum in the free-surfactant concentration. Because of these two latter effects of the salt and because of the fact that the surfactant binding isotherms are monotonously increasing functions of the free-surfactant concentration, the amount of surfactant bound to the polyelectrolyte molecules in the presence of excess surfactant decreases with increasing electrolyte concentration.

According to the previous reasoning, the impact of the electrolyte concentration on surfactant binding becomes much more pronounced with decreasing binding affinity of the surfactant.[4,5] However, it is also important to note that above a certain salt concentration the ionic surfactant becomes insoluble in the electrolyte solution, which therefore limits the further suppression of surfactant binding.[6−8]

The significant reduction in the bound amount of surfactant largely reduces the attractive dispersion forces acting between the PSS/CTAB nanoparticles, which explains the diminishing rate of their coagulation at high salt concentrations (as shown in Figure 4). At a certain electrolyte concentration, the bound amount of surfactant becomes so low that the system is converted from a colloidal dispersion of PSS/CTAB nanoparticles to a thermodynamically stable solution of the polyelectrolyte and

dx.doi.org/10.1021/la2021353 |Langmuir 2011, 27, 9139–9147

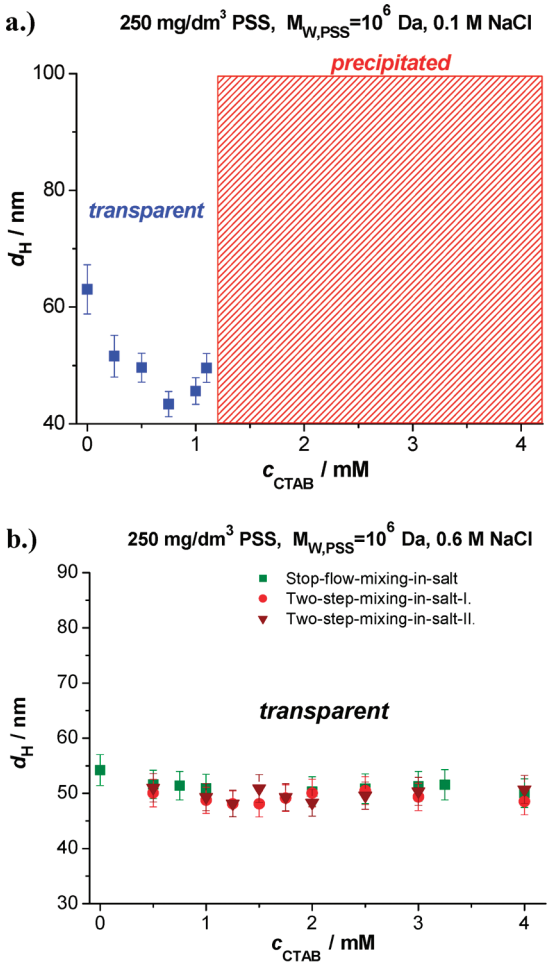

Figure 6. Variation of the phase properties of PSS/CTAB mixtures with an increasing surfactant-to-polyelectrolyte ratio (a) in 0.1 M NaCl and (b) in 0.6 M NaCl. The apparent mean hydrodynamic diameter of the PSS/CTAB complexes is also shown as a function of the analytical surfactant concentration. In 0.1 M NaCl, the mixtures were prepared via the stop-flow-mixing-in-salt protocol. In the presence of 0.6 M NaCl, the PSS/CTAB systems were prepared by three different mixing methods such as stop-flow-mixing-in-salt, two-step-mixing-in-salt-I, and two-step-mixing-in-salt-II mixing protocols. The details of these mixing procedures can be found in the Experimental Section. $M_{w,PSS}$ = 10^6 Da and c_{PSS}= 250 mg/dm^3.

surfactant molecules. Clearly, this type of salt effect is related to the equilibrium phase properties contrary to the previously proposed restabilization impact of added NaCl.

If the diminishing aggregation rate of the PSS/CTAB nanoparticles at high ionic strengths is attributable to the largely reduced surfactant binding, then an immediate enigma is why this effect of salt was not detected in polycation/SDS systems.[7,8] One of the possible answers is related to the observation that the driving force of surfactant binding is considerably lower for polyanion/cationic surfactant systems than for polycation/anionic surfactant mixtures at the same linear charge density of the polyelectrolytes and at the same alkyl chain length of the surfactants.[4,5] It is likely, therefore, that the salt-induced reduction of the bound amount of surfactant is more significant for the PSS/CTAB complexes than for the cationic polyelectrolyte/SDS complexes, which is also supported by surfactant binding studies.[25,35]

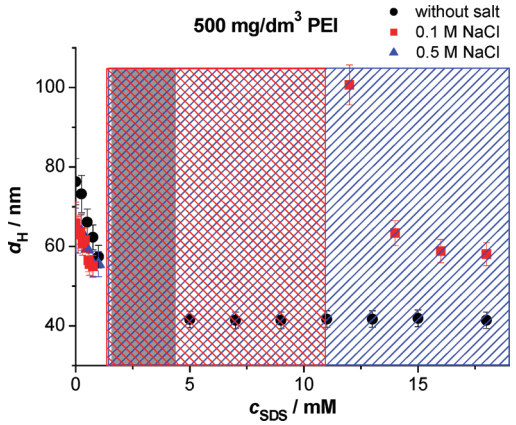

Figure 7. Apparent mean hydrodynamic diameter (d_H) of the PEI/SDS complexes as a function of the analytical surfactant concentration without NaCl (●) as well as in the presence of 0.1 (red ■) and 0.5 M (blue ▲) NaCl. c_{PEI} = 500 mg/dm^3. The measurements were carried out at pH^{in} 10, and the mixtures were prepared via the stop-flow-mixing-in-salt protocol. The gray area as well as the red and blue sparse areas indicates the composition range of precipitated systems without added salt as well as in the presence of 0.1 and 0.5 M NaCl, respectively.

Another important difference between the PSS/CTAB and polycation/SDS systems is connected to the different solubility of the surfactants in the NaCl medium. Although in the case of a 4 mM CTAB solution the surfactant remains soluble up to 1 M NaCl, precipitation can be observed for a 4 mM SDS solution at NaCl concentrations larger than 0.6 M.

The limited solubility of SDS in NaCl and its high binding affinity toward the cationic polyelectrolyte molecules prevent the considerable reduction of surfactant binding for the investigated polycation/SDS mixtures in the presence of salt. Therefore, in these latter mixtures the diminishing coagulation rate of the polycation/SDS nanoparticles formed in the presence of excess surfactant was not observed at high NaCl concentrations. Instead, as shown in Figure 5, at $c_{NaCl} \geq 0.6$ M the precipitation of SDS occurs in the polyelectrolyte-free solutions.

For the PSS/CTAB system, the surfactant binding affinity is lower compared to that of the polycation/SDS systems, and at the same time, CTAB is largely soluble in concentrated NaCl solutions. Therefore, the salt-induced suppression of surfactant binding is clearly observable for the PSS/CTAB mixtures at high salt concentrations, similar to that of other cationic surfactant/polyanion systems.[4−6,10−13]

Effect of Salt on the Phase Properties of PSS/CTAB Systems. In Figure 6a,b, the variation of the apparent mean size of the PSS/CTAB complexes with increasing analytical surfactant concentration is shown for mixtures prepared by the stop-flow mixing-in-salt protocol in the presence of 0.1 and 0.6 M NaCl, respectively (c_{PSS} = 250 mg/dm^3, $M_{w,PSS}$ = 10^6 Da). Similar graphs for the two other concentrations of the high-molecular-mass PSS sample and for the same monomer concentration of the low-molecular-mass PSS sample can be seen in Figures S5−S7 in the Supporting Information.

According to Figures 6 and S5−S7 in 0.1 M NaCl, transparent systems are formed only in the presence of excess polyelectrolyte where the apparent mean size of the complexes decreases as a function of the surfactant concentration. Contrary to the observations in the absence of salt (shown in Figures 1a−c and 2), precipitation occurs not only at the intermediate CTAB concentrations but also

dx.doi.org/10.1021/la2021353 |*Langmuir* 2011, 27, 9139–9147

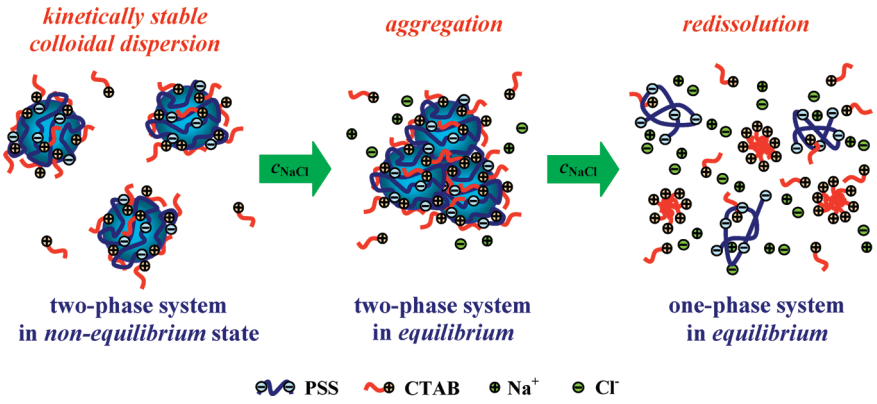

Figure 8. Schematic illustration of the effect of increasing salt concentration on the polyelectrolyte/surfactant association in the charge-stabilized colloidal dispersion regime. The blue spheres denote the hydrophobic cores of polyelectrolyte/surfactant nanoparticles that contain large numbers of bound surfactant ions.

over the whole investigated concentration range of excess surfactant. In this case, even the application of very rapid stop-flow-mixing cannot prevent the aggregation of the PSS/CTAB nanoparticles, which is highly accelerated at this electrolyte concentration.

In the presence of 0.6 M NaCl, transparent systems with very low turbidity are formed in the investigated surfactant concentration range at each polyelectrolyte concentration of the two PSS samples. At this salt concentration, the apparent mean size of the PSS/CTAB complexes does not depend considerably on the surfactant or polyelectrolyte concentration ($d_H \approx 51 \pm 3$ nm at the three applied concentrations of the high-molecular-mass PSS sample and $d_H \approx 14 \pm 2$ nm for the low-molecular-mass PSS sample at c_{PSS} = 250 mg/dm^3) in the investigated composition range. A few measurements were also carried out in PSS/CTAB systems prepared in the presence of 0.8 M NaCl at 500 mg/dm^3 concentration of the high-molecular-mass PSS sample (data not shown). The apparent mean size of the complexes at a given surfactant concentration was the same within the experimental error as in the presence of 0.6 M NaCl.

To test the thermodynamic stability of the PSS/CTAB systems at high salt concentrations, the reversibility of the complexation was also investigated through the application of two other solution-preparation methods in addition to the previously mentioned stop-flow mixing-in-salt protocol. In these mixing methods, the final state of the system (c_{PSS} = 250 mg/dm^3 and c_{NaCl} = 0.6 M) was attained in two steps. First, the polyelectrolyte/surfactant mixtures were prepared in the absence of salt by the slow-mixing protocol, and then the systems were left to stand for a day. Next, these systems were mixed either with a 1.2 M NaCl solution in equal volumes (two-step-mixing-in-salt-I protocol) or a calculated amount of solid NaCl crystals were added to the PSS/CTAB mixtures and they were stirred with a magnetic stirrer (two-step-mixing-in-salt-II protocol). In the Supporting Information, Scheme 1 illustrates through a specific example how the final composition was attained by making use of the three different mixing methods.

It is important to note that under constant ionic strength (stop-flow-mixing-in-salt procedure) both the initial PSS and CTAB solutions and the final mixtures were transparent in the investigated composition range. In contrast, in the case of the other two mixing methods, precipitation was observed over a wide composition range during the first step of the mixing procedure (slow-mixing), in accordance with the findings in Figures 3 and S2−S4. These precipitates, however, were dissolved immediately upon addition of the salt. Furthermore, as shown in Figure 6b, the apparent mean size of the complexes at a given composition is not dependent on the applied mixing methods within the experimental error.

This also means that the transparent PSS/CTAB systems formed in the presence of 0.6 M NaCl are thermodynamically stable solutions of the polyelectrolyte and surfactant molecules. This finding can be rationalized by the largely reduced amount of surfactant bound to the polyelectrolyte molecules, which also explains the considerably reduced coagulation rate of the PSS/CTAB nanoparticles in the presence of high NaCl concentrations (Figure 4a,b).

The results presented in Figures 6 and S5−S7 are in sharp contrast to the recently observed impact of added salt on cationic polyelectrolyte/SDS systems prepared via the stop-flow-mixing protocol.[7,8] One example is shown in Figure 7, where the apparent mean hydrodynamic diameter of the PEI/SDS complexes is plotted as a function of the analytical surfactant concentration without salt as well as in the presence of 0.1 and 0.5 M NaCl. Similar to the earlier investigated polycation/SDS mixtures, the primary effect of the added electrolyte on the PEI/SDS system is the enhancement of the precipitation concentration range even at such a high salt concentration as 0.5 M NaCl. This is attributable to the accelerated coagulation of the primary PEI/SDS nanoparticles in which the bound amount of surfactant is not reduced largely even upon addition of 0.5 M NaCl. A salt-induced suppression of the associative phase separation cannot be detected because at even larger salt concentrations the precipitation of SDS (segregative phase separation) occurs.[7,8]

CONCLUSIONS

In the presence of excess surfactant, the application of the stop-flow-mixing protocol results in a colloidal dispersion of positively charged PSS/CTAB nanoparticles that are aggregates of the individual PSS/CTAB complexes. The average number of primary complexes in these polyelectrolyte/surfactant aggregates as well as the precipitation concentration range increases with increasing analytical concentration or (at fixed monomer concentration) with decreasing molecular mass of the PSS samples.

We have shown that two distinct effects of the added salt on the polyelectrolyte/surfactant association have to be distinguished, which are illustrated in Figure 8. The major impact of

dx.doi.org/10.1021/la2021353 |*Langmuir* 2011, 27, 9139–9147

the added electrolyte at moderate salt concentrations is manifested in the reduction of the composition range in which the mixtures are trapped in the charge-stabilized colloidal dispersion state. This effect of the added salt can be detected only when the experimental conditions facilitate the formation of electrostatically stabilized polyelectrolyte/surfactant dispersions in the absence of salt. At higher salt concentrations, the presence of electrolyte primarily affects the equilibrium phase properties by considerably decreasing the surfactant binding and suppressing the associative phase separation. This latter effect of the salt is observable only when the driving force of surfactant binding is low and the amphiphile is largely soluble even in very concentrated electrolyte solutions.

The presented results offer interesting possibilities for future applications. For instance, a charge-stabilized colloidal dispersion of polyelectrolyte/surfactant aggregates may solubilize large numbers of apolar substances in their hydrophobic interior, which can be released by a sudden increase in the electrolyte concentration. Similarly, via surface deposition of these nanoparticles, the hydrophobicity of the given interface may be tuned with the variation in the ionic strength of the surrounding medium. Further studies are in progress in order to explore these potential applications.

■ ASSOCIATED CONTENT

Supporting Information. Additional experimental information as discussed in the text. This material is available free of charge via the Internet at http://pubs.acs.org.

■ AUTHOR INFORMATION

Corresponding Author
*E-mail: meszaros@chem.elte.hu.

■ ACKNOWLEDGMENT

This work was supported by the European Commission under COST Action D43 as well as by the Hungarian Scientific Research Fund (OTKA K 81380), which is gratefully acknowledged.

■ REFERENCES

(1) Goddard, E. D., Ananthapadmanabhan, K. P., Eds. *Interactions of Surfactants with Polymers and Proteins*; CRC Press: Boca Raton, FL, 1993; Chapter 4.
(2) Marchioretto, S.; Blakely, J. *SOFW J.* **1997**, *123*, 811–818.
(3) Rodriguez, R.; Alvarez-Lorenzo, C.; Concheiro, A. *Eur. J. Pharm. Sci.* **2003**, *20*, 429–438.
(4) Thalberg, K.; Lindman, B.; Bergfeldt, K. *Langmuir* **1991**, *7*, 2893–2898.
(5) Thalberg, K.; Lindman, B.; Karlström, G. *J. Phys. Chem.* **1991**, *95*, 3370–3376.
(6) Thalberg, K.; Lindman, B.; Karlström, G. *J. Phys. Chem.* **1991**, *95*, 6004–6011.
(7) Mezei, A.; Ábrahám, Á.; Pojják, K.; Mészáros, R. *Langmuir* **2009**, *25*, 7304–7312.
(8) Ábrahám, Á.; Mezei, A.; Mészáros, R. *Soft Matter* **2009**, *5*, 3718–3726.
(9) Voisin, D.; Vincent, B. *Adv. Colloid Interface Sci.* **2003**, *106*, 1–22.
(10) Wang, X.; Li, Y.; Li, J.; Wang, J.; Wang, Y.; Guo, Z.; Yan, H. *J. Phys. Chem B* **2005**, *109*, 10807–10812.
(11) Pi, Y.; Shang, Y.; Liu, H.; Hu, Y.; Jiang, J. *J. Colloid Interface Sci.* **2007**, *306*, 405–410.
(12) Liu, J.; Zheng, L.; Sun, D.; Wei, X. *Colloids Surf., A* **2010**, *358*, 93–100.
(13) Matsuda, T.; Annaka, M. *Langmuir* **2008**, *24*, 5707–5713.
(14) Pispas, S. *J. Phys. Chem. B* **2007**, *111*, 8351–8359.
(15) Mantzaridis, C.; Mountrichas, G.; Pispas, S. *J. Phys. Chem. B* **2009**, *113*, 7064–7070.
(16) Wang, Y.; Kimura, K.; Huang, Q. R.; Dubin, P. L.; Jaeger, W. *Macromolecules* **1999**, *32*, 7128–7134.
(17) Piculell, L.; Lindman, B. *Adv. Colloid Interface Sci.* **1992**, *41*, 149–178.
(18) Ilekti, P.; Piculell, L.; Tournilhac, F.; Cabane, B. *J. Phys. Chem. B* **1998**, *102*, 344–351.
(19) Santos, O.; Johnson, E. S.; Nylander, T.; Panandiker, R. K.; Sivik, M. R.; Piculell, L. *Langmuir* **2010**, *26*, 9357–9367.
(20) Santos, S.; Gustavsson, C.; Gudmundsson, C.; Linse, P.; Piculell, L. *Langmuir* **2011**, *27*, 592–603.
(21) Mezei, A.; Mészáros, R.; Varga, I.; Gilányi, T. *Langmuir* **2007**, *23*, 4237–4247.
(22) Mezei, A.; Pojják, K.; Mészáros, R. *J. Phys. Chem. B* **2008**, *112*, 9693–9699.
(23) Mészáros, R.; Thompson, L.; Bos, M.; Varga, I.; Gilányi, T. *Langmuir* **2003**, *19*, 609–615.
(24) Oster, G. *J. Colloid Sci.* **1960**, *15*, 512.
(25) Mezei, A.; Mészáros, R. *Langmuir* **2006**, *22*, 7148–7151.
(26) Naderi, A.; Claesson, P. M.; Bergström, M.; Dedinaite, A. *Colloids Surf., A* **2005**, *253*, 83–93.
(27) Naderi, A.; Claesson, P. M. *J. Dispersion Sci. Technol.* **2005**, *26*, 329–340.
(28) Tonigold, K.; Varga, I.; Nylander, T.; Campbell, R. A. *Langmuir* **2009**, *25*, 4036–4046.
(29) Campbell, R. A.; Angus-Smyth, A.; Arteta, M. Y.; Tonigold, K.; Nylander, T.; Varga, I. *J. Phys. Chem. Lett.* **2010**, *1*, 3021–3026.
(30) Mezei, A.; Mészáros, R. *Soft Matter* **2008**, *4*, 586–593.
(31) Pojják, K.; Mészáros, R. *Langmuir* **2009**, *25*, 13336–13339.
(32) Claesson, P. M.; Bergström, M.; Dedinaite, A.; Kjellin, M.; Legrand, J. F.; Grillo, I. *J. Phys. Chem. B* **2000**, *104*, 11689–11694.
(33) Israelachvili, J. N.; Adams, G. E. *J. Chem. Soc., Faraday Trans.* **1978**, *74*, 975.
(34) Lopez-Leon, T.; Gea-Jodar, P. M.; Bastos-Gonzalez, D.; Ortega-Vinuesa, J. L. *Langmuir* **2005**, *21*, 87–93.
(35) Hayakawa, K.; Kwak, J. C. T. *J. Phys. Chem.* **1982**, *86*, 3866–3870.
(36) Hansson, P.; Almgren, M. *J. Phys. Chem.* **1996**, *100*, 9038–9046.
(37) Hansson, P. *Langmuir* **2001**, *17*, 4167–4180.
(38) Donati, I.; Borgogna, M.; Turello, E.; Cesaro, A.; Paoletti, S. *Biomacromolecules* **2007**, *8*, 1471–1479.